Indian Journal of Chemistry
Vol. 64, April 2025, pp. 383-390
DOI: 10.56042/ijc.v64i4.15530

Molecular docking and dynamic simulation of anti-apoptotic BCL-2 with saponins isolated from *Weigela* x "Bristol Ruby"

Hung Duc Nguyen
Thai Nguyen University of Education, 24000, Thai Nguyen, Vietnam
E-mail: hungnd@tnue.edu.vn

Received 4 December 2024; accepted (revised) 26 March 2025

Colon cancer is the second leading cause of cancer-related deaths worldwide. Apoptosis may play a key role in the tissue mass homeostasis of the colonic mucosa. The B-cell lymphoma-2 (BCL-2) family plays an important role in determining the decision to undergo apoptosis. A previous study revealed the potential cytotoxicity on colorectal cancer cell line of triterpenoid saponins isolated from *Weigela* x "Bristol Ruby". In this *in silico* study, triterpenoid saponins from *W.* x "Bristol Ruby" have been studied for their inhibition potential using molecular docking on the 6GL8 receptor. All compounds exhibit hydrogen bonds, Van der Waals, and hydrophobic interactions in molecular docking. The binding potentials of triterpenoid saponins and a reference compound, 5-FU, as target protein 6GL8 have been examined using molecular docking. Among of those, 3-*O*-β-D-xylopyranosyl-(1→4)-β-D-glucopyranosyl-(1→4)-β-D-xylopyranosyl-(1→3)-α-L-rhamnopyranosyl-(1→2)-α-L-arabinopyranosyloleanolic acid (CPD1) binds to the 6GL8 receptor with the highest binding stabilities at –5.08 kcal/mol, in comparison with the reference 5-FU at –3.59 kcal/mol. Molecular dynamic studies have been further conducted to better comprehend ligands' dynamics within the target protein's binding pocket. The result show that the binding of CPD1 to the 6GL8 receptor is stable throughout the simulation. CPD1 could be a good candidate for new inhibitors of anti-apoptotic BCL-2 proteins in colorectal cancer.

Keywords: Colorectal cancer, *Weigela* x "Bristol Ruby", Molecular docking, Molecular dynamic simulation, Triterpenoid saponin

Cancer is a group of diseases that is characterized by uncontrolled cell proliferation. This unconstrained cell growth has the potential to invade nearby and distant tissues, causing life-threatening complications[1]. Colon cancer is the second leading cause of cancer-related deaths worldwide, with more than 1.9 million new cases and more than 930 000 deaths due to colorectal cancer in 2020. Apoptosis may play a key role in the tissue mass homeostasis of the colonic mucosa. It is observed in controlled deletion of cells during metamorphosis, differentiation, and general cell turnover and usually appears regulated by receptor-coupled events. For these reasons, apoptosis has been called "programmed cell death" or "cell suicide"[2]. There are two main apoptotic pathways, which are the extrinsic pathway and the intrinsic pathway[3]. The Bcl-2 protein family regulates the main process of apoptosis in the intrinsic pathway. In cancer, over-expression of the anti-apoptotic protein Bcl-2 allows an inhibition of the intrinsic apoptotic[4,5].

The *Weigela* genus contains ten accepted species distributed mainly in China to Russian Far East and Japan, but over 200 cultivars have been produced in the world[6]. Previous studies on some species of the *Weigela* genus revealed the presence of triterpenoid saponins possessing potential cytotoxic properties against cancer cell lines[6–9]. Triterpenoid saponins have been studied for a wide range of biological activities, including anti-tumor, cytotoxic, antibacterial, anti-inflammatory, and antioxidant properties[10]. As an anti-tumor agent, triterpenoid saponins have various molecular mechanisms which can induce apoptosis through the inhibition of anti-apoptotic protein Bcl-2 (Ref. 11). Previous studies on *Weigela* x "Bristol Ruby" resulted in the isolation of triterpenoid saponins possessing potent cytotoxicity, but their inhibitory properties to apoptosis have not been screened[8]. In this study, molecular docking and dynamic simulation were carried out on the triterpenoid saponins isolated from *W.* x "Bristol Ruby" as inhibitors of the anti-apoptotic protein Bcl-2 in colorectal cancer to determine the mechanism of their anticancer potency before carrying out *in vitro* experiments.

Experimental Section

Protein preparation

The three-dimensional structure of target BCL-2 (code ID: 6GL8) was extracted from RCSB Protein

Data Bank (https://www.rcsb.org/) in .pdb format[12]. The preparation process involved preparing receptors and removing water molecules using Biovia Discovery Studio Visualizer v24.1 (Dassault Systemes BIOVIA, USA). Appropriate binding orientations and conformations of the ligand molecules with protein inhibitors were performed using AutoDock Tools v1.5.7 (Center for Computational Structural Biology, USA). All co-crystalized ligands were cut from the protein complexes and used to validate the molecular docking protocol by calculating root mean square deviation (RMSD) using Biovia Discovery Studio Visualizer. After the protein was cleaned, only polar hydrogens and the Kollman charges were introduced.

Ligand preparation

Five triterpenoid saponins possessing potent cytotoxicities against a mouse colon cancer cell line CT26 were retrieved from the previous study[8]. For details, these saponins including 3-*O*-β-D-xylopyranosyl-(1→4)-β-D-glucopyranosyl-(1→4)-β-D-xylopyranosyl-(1→3)-α-L-rhamnopyranosyl-(1→2)-α-L-arabinopyranosyloleanolic acid (CPD1); 3-*O*-β-D-xylopyranosyl-(1→4)-[β-D-glucopyranosyl-(1→3)]-β-D-glucopyranosyl-(1→4)-β-D-xylopyranosyl-(1→3)-α-L-rhamnopyranosyl-(1→2)-α-L-arabinopyranosyloleanolic acid (CPD2); 3-*O*-β-D-xylopyranosyl-(1→4)-[α-L-arabinopyranosyl-(1→3)]-β-D-glucopyranosyl-(1→4)-β-D-xylopyranosyl-(1→3)-α-L-rhamnopyranosyl-(1→2)-arabinopyranosyloleanolic acid (CPD3); 3-*O*-β-D-xylopyranosyl-(1→4)-β-D-glucopyranosyl-(1→4)-β-D-xylopyranosyl-(1→3)-α-L-rhamnopyranosyl-(1→2)-β-D-xylopyranosyloleanolic acid 28-*O*-β-D-glucopyranosyl ester (CPD6); 3-*O*-β-D-xylopyranosyl-(1→4)-β-D-glucopyranosyl-(1→4)-β-D-xylopyranosyl-(1→3)-α-L-rhamnopyranosyl-(1→2)-β-D-xylopyranosyloleanolic acid (CPD7), have molecular formulas of $C_{57}H_{92}O_{24}$, $C_{63}H_{102}O_{29}$, $C_{62}H_{100}O_{28}$, $C_{63}H_{102}O_{29}$, $C_{57}H_{92}O_{24}$, and molecular weights of 1160.5979, 1322.6507, 1292.6402, 1322.6507, 1160.5979 *m/z*, respectively. The 2D structures of five triterpenoid saponins were prepared in .sdf format using ChemDraw Prime v23.1 (Perkin Elmer, USA) and further converted to 3D structures in .pdb format using Biovia Discovery Studio Visualizer. Only polar hydrogens and the Compute Gasteiger were also added, and all torsions were allowed to rotate by performed using AutoDock Tools. The 2D structure of Fluorouracil (5-FU) was obtained from the PubChem database in .sdf format (https://pubchem.ncbi.nlm.nih.gov) and further converted to .pdb format using Biovia Discovery Studio Visualizer.

Molecular docking

Molecular docking between ligands and receptors was carried out based on the mode of action using the AutoDock Tools application. The Lamarckian genetic algorithm determined the most energy-favorable ligand-protein binding conformations. All parameters were set to default except for the genetic algorithm runs. 5-FU was chosen as the control ligand.

Molecular dynamic simulation

Molecular dynamic simulation for the best-docked confirmation with 6GL8 protein was performed for 100 ns using GROMACS v2024.1 software[13]. The protein was fixed to avoid missing atoms and residues using Swiss-PdbViewer software[14]. Swiss PARAM was used to produce the topologies of ligands[15]. For the solvation system, a triclinic simulation box fitting the protein-ligand complex was generated by the SPC water model. 0.15 M sodium chloride has been added to the system. The energy minimization and neutralization for structure optimizations were set at 50000 steps. The system was equilibrated at 300 K temperature and 1.0 bar pressure. The performance of the simulation was set at 150000 steps. The equilibrated system is set for the molecular dynamic simulation run up to 50000 steps per 100 ps on an Intel(R) Xeon(R) CPU @ 2.20GHz computer equipped with a GPU NVIDIA Tesla T4 16GB GDDR6. The molecular dynamic simulation data were analyzed at 100 ns using UCSF Chimera v1.17.3 and Grace software (Grace Development Team)[16]. The simulation data was analyzed for the number of hydrogen bonds (H-bonds) in each frame over time, root mean square fluctuation (RMSF) of each residue in the given structure, and RMSD of the given structure over time.

Results and Discussion

In the present study, five triterpenoid saponins were obtained from *W.* x "Bristol Ruby" and screened through molecular docking against the targeted protein 6GL8 (Fig. 1). Each of the generated docked complexes was observed centered on minimum binding energy values (kcal/mol). The interactions of the ligands within the binding pockets of 6GL8 are

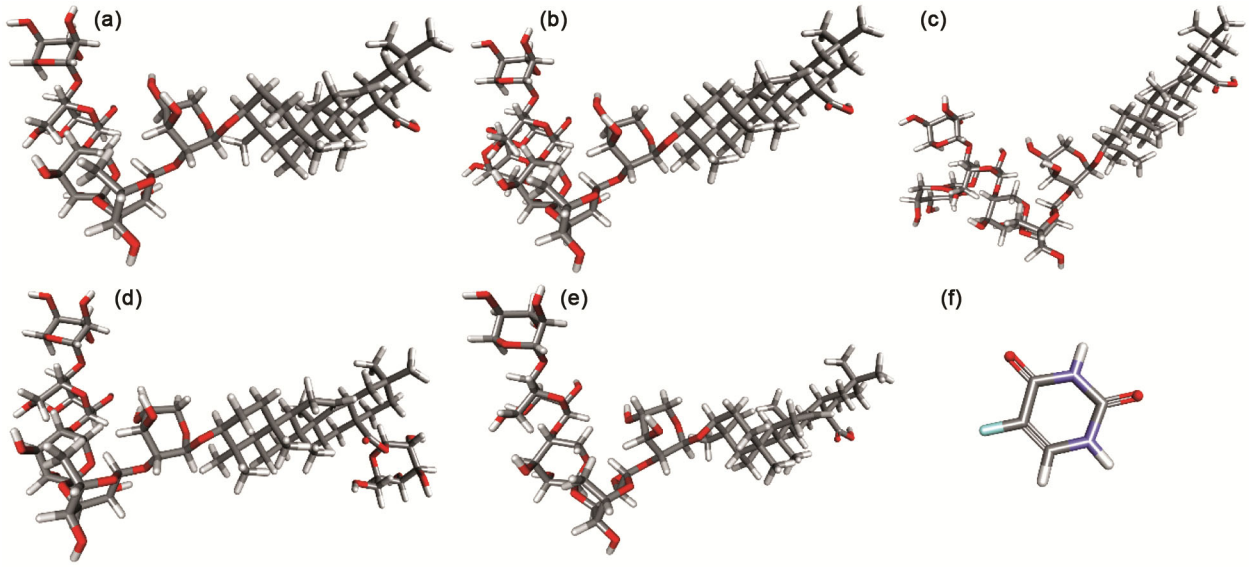

Fig. 1 — 3D structure of the tested ligands. (A) 3-O-β-D-xylopyranosyl-(1→4)-β-D-glucopyranosyl-(1→4)-β-D-xylopyranosyl-(1→3)-α-L-rhamnopyranosyl-(1→2)-α-L-arabinopyranosyloleanolic acid (CPD1); (B) 3-*O*-β-D-xylopyranosyl-(1→4)-[β-D-glucopyranosyl-(1→3)]-β-D-glucopyranosyl-(1→4)-β-D-xylopyranosyl-(1→3)-α-L-rhamnopyranosyl-(1→2)-α-L-arabinopyranosyloleanolic acid (CPD2); (C) 3-*O*-β-D-xylopyranosyl-(1→4)-[α-L-arabinopyranosyl-(1→3)]-β-D-glucopyranosyl-(1→4)-β-D-xylopyranosyl-(1→3)-α-L-rhamnopyranosyl-(1→2)-arabinopyranosyloleanolic acid (CPD3); (D) 3-*O*-β-D-xylopyranosyl-(1→4)-β-D-glucopyranosyl-(1→4)-β-D-xylopyranosyl-(1→3)-α-L-rhamnopyranosyl-(1→2)-β-D-xylopyranosyloleanolic acid 28-*O*-β-D-glucopyranosyl ester (CPD6); (E) 3-*O*-β-D-xylopyranosyl-(1→4)-β-D-glucopyranosyl-(1→4)-β-D-xylopyranosyl-(1→3)-α-L-rhamnopyranosyl-(1→2)-β-D-xylopyranosyloleanolic acid (CPD7); (F) 5-FU.

Table 1 — The interactions between the docked ligands and the protein 6GL8

Docked ligands	Binding energy (kcal/mol)	Hydrogen bond interaction	Van der Waals interaction	Hydrophobic interaction
CPD1	–5.08	ARG106, ARG107, ARG110, ARG146, ASP103	ALA100, ARG109, GLY145, TYR108, VAL148	PHE104, TYR202
CPD2	–1.02	ARG146, ASP111, GLN118	ASP140, GLU114, GLU136, LEU119, MET115, PHE153, TYR108	LEU137, VAL133
CPD3	–3.22	ARG146, GLN118, GLU136	ALA149, ASP111, LEU137, PHE112, PHE153, VAL133	LEU119, MET115, PHE104, TYR108
CPD6	–0.87	ARG107, GLU136, GLY145, TYR202, ASN143	ARG146, ASP111, GLN118, GLU114, LEU119, LEU137, LEU201, MET115, PHE153, TRP144, VAL133	ALA149, PHE104, PHE112, TYR108, TYR202
CPD7	–5.07	ARG146, GLN118, LEU119	ALA149, ASN143, ARG107, ARG129, GLU136, GLY145, HIS120, LEU119, LEU137, MET115, PHE112, PHE153,	LEU201, PHE104, TRP144, TYR108, TYR202
5-FU	–3.59	ALA100, ARG107, GLY145, TYR202	ARG106, ASP103	PHE104, VAL148

shown in Table 1. The amino acid residues involved in the interactions and their position in their ligand-binding site were identified. Hydrogen bonds, Van der Waals, and hydrophobic interactions between the protein and the ligands were demonstrated through molecular docking. Each specific molecular interaction with the amino acids of 6GL8 was demonstrated in Fig. 2. CPD1, CPD2, CPD3, CPD6, CPD7, and 5-FU exhibited unbounded weak molecular interactions such as Van der Waals forces. For details, CPD1 displayed Van der Waals forces with amino acid residues ALA100, ARG109, GLY145, TYR108, and VAL148 of 6GL8. For CPD2, seven amino acid residues including ASP140, GLU114, GLU136, LEU119, MET115, PHE153 and TYR108 showed Van der Waals interaction. CPD3 showed Van der Waals interaction with amino acid residues ALA149, ASP111, LEU137, PHE112,

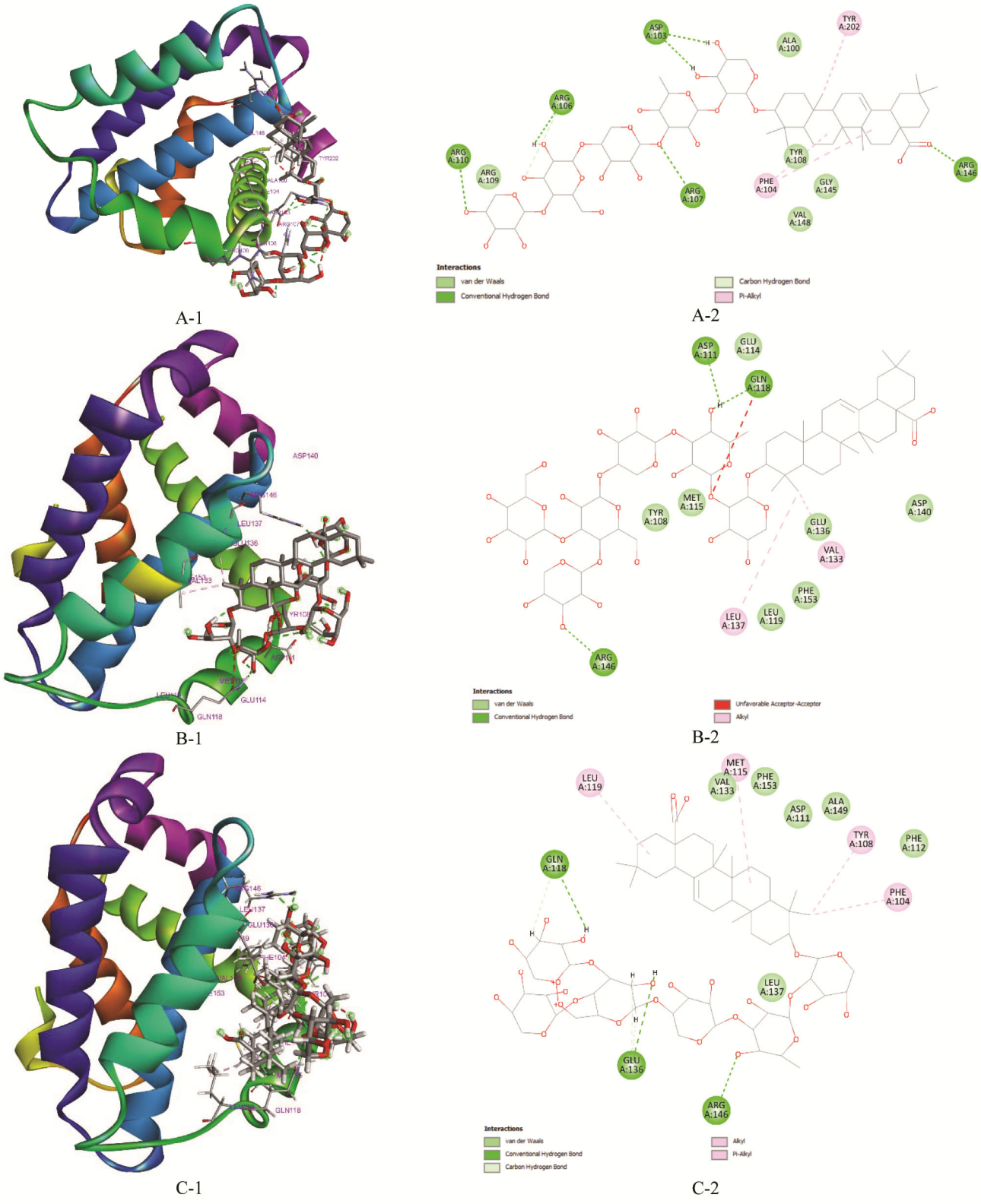

Fig. 2 — Molecular docking model and 2D interaction diagram of CPD1 (A-1, A-2), CPD2 (B-1, B-2), CPD3 (C-1, C-2), CPD6 (D-1, D-2), CPD7 (E-1, E-2) and 5-FU (F-1, F-2) against 6GL8 protein receptor.

(*Contd*.)

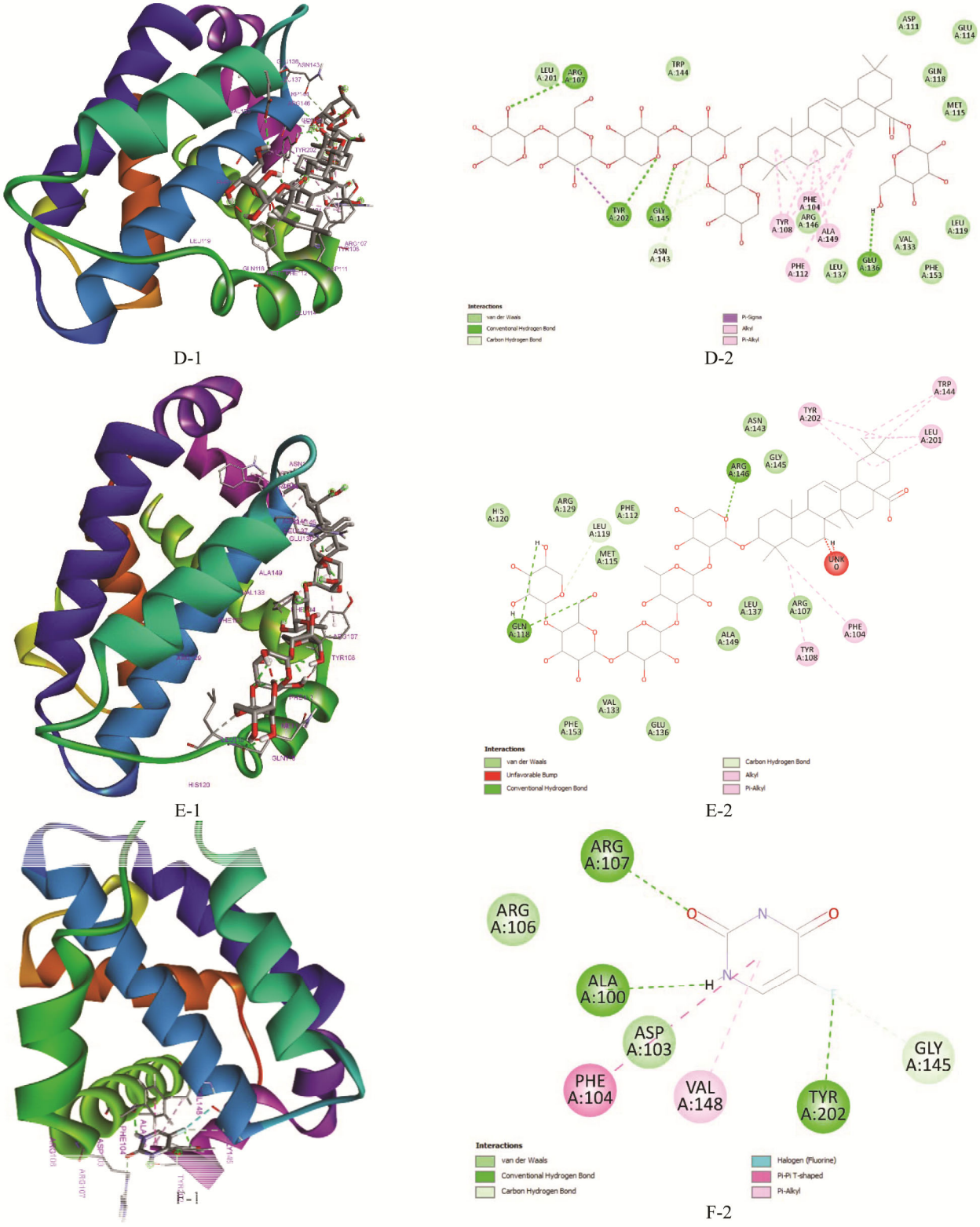

Fig. 2 — Molecular docking model and 2D interaction diagram of CPD1 (A-1, A-2), CPD2 (B-1, B-2), CPD3 (C-1, C-2), CPD6 (D-1, D-2), CPD7 (E-1, E-2) and 5-FU (F-1, F-2) against 6GL8 protein receptor.

PHE153, and VAL133. CPD6 interacts with 6GL8 through Van der Waals interaction with amino acid residues ARG146, ASP111, GLN118, GLU114, LEU119, LEU137, LEU201, MET115, PHE153, TRP144, and VAL133. For CPD7, twelve amino acid residues including ALA149, ASN143, ARG107, ARG129, GLU136, GLY145, HIS120, LEU119, LEU137, MET115, PHE112, and PHE153 showed Van der Waals interaction. Lastly, 5-FU, the comparative ligand, exhibited Van der Waals forces to specific amino acid residues ARG106 and ASP103. Interestingly, Van der Waals interactions create high material functionalities, determine the formation of the protein-ligand complex, distinguish the compound's fine structures, and stabilize the protein complexes[17,18].

Bounded strong molecular interactions such as hydrogen bonds and hydrophobic interactions are also seen in each ligand aside from Van der Waals forces. Hydrogen bonds were found in the interaction of CPD1 with the amino acid residues ARG106, ARG107, ARG110, ARG146 and ASP103 (Fig. 2A-1); CPD2 with the amino acid residues ARG146, ASP111 and GLN118 (Fig. 2B-1). CPD3 exhibited hydrogen bond interactions with the amino acid residues ARG146, GLN118 and GLU136 (Fig. 2C-1); CPD6 with the amino acid residues ARG107, GLU136, GLY145, TYR202 and ASN143 (Fig. 2D-1); CPD7 with the amino acid residues ARG146, GLN118 and LEU119 (Fig. 2E-1). 5-FU exhibited hydrogen bond interactions with the amino acid residues ALA100, ARG107, GLY145 and TYR202 (Fig. 2F-1). On the other hand, CPD1 formed hydrophobic interactions with the receptor residues PHE104 and TYR202 and CPD2 with the amino acid residues LEU137 and VAL133. CPD3 exhibited interactions with the amino acid residues LEU119, MET115, PHE104 and TYR108; CPD6 with the amino acid residues ALA149, PHE104, PHE112, TYR108 and TYR202; CPD7 with the amino acid residues LEU201, PHE104, TRP144, TYR108 and TYR202. 5-FU exhibited hydrophobic interactions with the amino acid residues PHE104 and VAL148.

Hydrogen bond interactions play an important role in stabilizing the ligand-protein complex[19]. CPD1 exhibited hydrogen bonding as it interacts with amino acids ARG106, ARG107, ARG110, ASP103, and ARG146 at the active sites of 6GL8 (Fig. 2A-2). Hydrogen bonds positively correlate to protein-ligand stability, which gives CPD1 good binding stability (–5.08 kcal/mol). In the case of CPD7, three hydrogen bondings interact with GLN118, LEU119, and ARG146 at the active sites of 6GL8 (Fig. 2E-2). The ARG and ASP are polar amino acids with high propensities (P_a = 3.18, 1.43, respectively). Common features of the amino acids with high propensity are that they are hydrophilic and contain highly electronegative atoms in the outermost region of their side chains[20]. This reason led to CPD1 possessing good binding stability (–5.08 kcal/mol) (Table 1). In the case of CPD7, the binding stability is –5.07 kcal/mol, which is almost the same as CPD1. This could be explained by the presence of a nonpolar amino acid, LEU, and two polar amino acids, ARG and GLU, which can form multiple hydrogen bonds[20,21]. On the other hand, CPD3 exhibited three hydrogen bondings as it interacted with amino acids ARG146, GLN118, and GLU136, resulting in good binding stability (–3.22 kcal/mol) (Fig. 2C-2). In the case of CPD6, the interaction of five hydrogen bondings with amino acids ARG107, GLU136, GLY145, TYR202, and ASN143 possess the lowest binding stability (–0.87 kcal/mol) (Fig. 2D-2). 5-FU exhibited four hydrogen bonds as it interacted with amino acids ALA100, ARG107, GLY145, TYR202 and two hydrophobic interactions with amino acids PHE104, VAL148 possessing a good binding stability (–3.59 kcal/mol) (Fig. 2F-2). Terefe *et al*. (2022) stated that the higher the bond affinity between the receptor and the ligand is, the more negative the binding affinity[22]. So, CPD1 is more stabilized than the other triterpenoid saponins because this compound has stronger molecular interactions and the highest binding stability. So, molecular dynamic studies were conducted to better understand ligand dynamics within the target protein's binding pocket. These experiments focused on active CPD1 with 6GL8, in which the starting point was set as the ligand-protein complex structures derived from the docking studies. A molecular dynamic simulation of the complex between 5-FU and 6GL8 was performed to provide a comparison.

The total energy and potential values obtained in the molecular dynamic simulation for CPD1 were calculated as –223,622 and –278,677 kJ/mol, respectively. Compared to the reference 5-FU, the total energy and potential values obtained in the molecular dynamic simulation for 5-FU were calculated as –231,601 and –286,339 kJ/mol, respectively. The system had been equilibrated for 300 K temperature. RMSD value was conducted to examine the stability of the protein backbone[23]. The RMSD value for the CPD1-6GL8 complex gradually increased from 0.11 to 0.22 nm during the initial stages of the molecular dynamic simulation until 2 ns

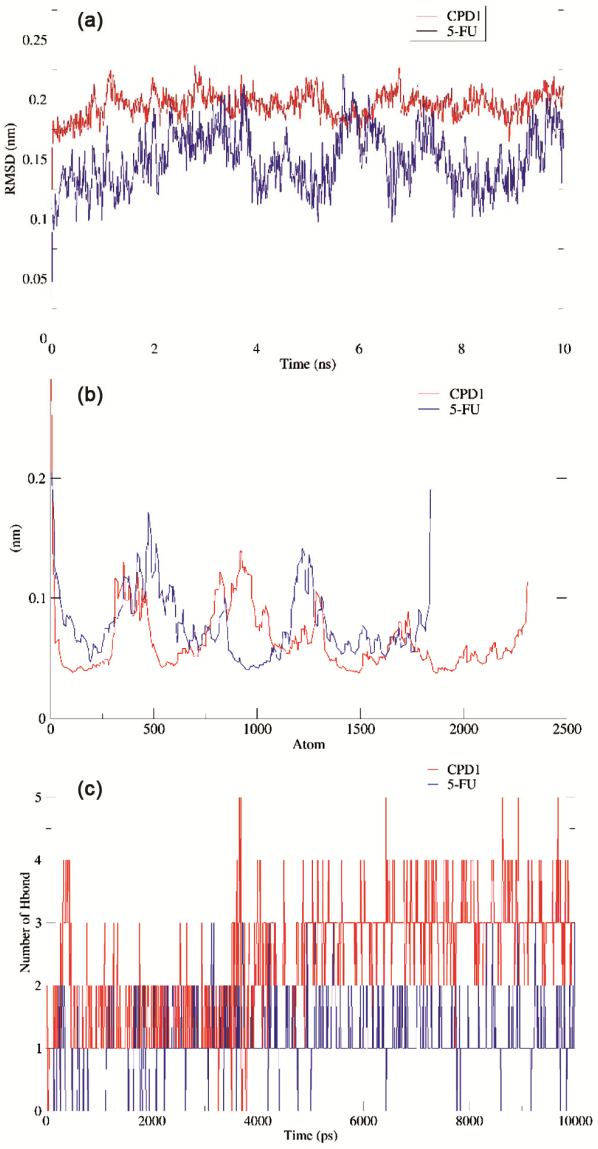

Fig. 3 — Results of MD simulation for the bindings of CPD1 (red) and 5-FU (blue) with 6GL8 protein. (A) RMSD, (B) RMS fluctuation, (C) The number of hydrogen bonds.

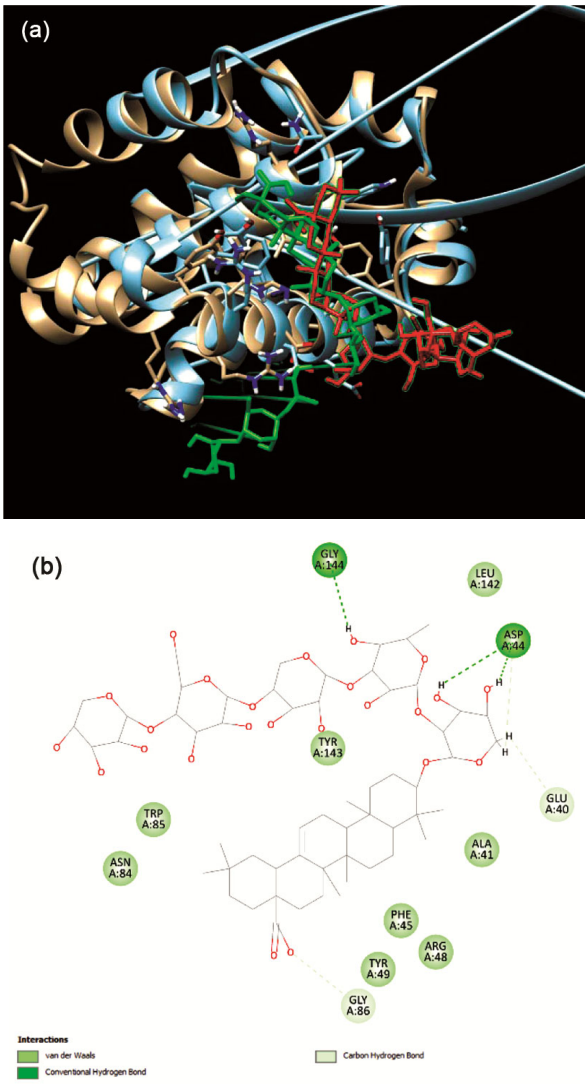

Fig. 4 — (A) Structural superposition of CPD1 and 6GL8 docked complex before molecular dynamic (0 ps, green) and after molecular dynamic (10000 ps, red). (B) Interactions schematic after 10000 ps molecular dynamic simulation.

of calibration and subsequently stabilized, maintaining an average RMSD of 0.2 nm throughout the remainder of the MD trajectory. The RMSD value of the complex of 5-FU and 6GL8 showed that the position did not change much once the ligands stabilized (Fig. 3A). The potential fluctuations of residues in protein backbone was identified by the RMSF value, which exhibited the same 0.15 nm both the CPD1-6GL8 complex and the complex of 5-Fu and 6GL8 (Fig. 3B). Hydrogen bonds were observed throughout the simulation, showing 1-5 hydrogen bonds consistently formed in the CPD1-6GL8 complex and 1-3 hydrogen bonds consistently formed in the complex of 5-FU and 6GL8. These results indicated CPD1 remained within the binding pocket for the entire simulation and stronger than 5-FU (Fig. 3C). The superposition of CPD1 with the binding pocket of 6GL8 before and after the molecular dynamic simulation (Fig. 4A). After 10000 ps of molecular dynamic simulation, hydrogen bonds were showed between CPD1 and 6GL8, including ASP44, GLU40, GLY86, GLY144. Additionally, Van der Waals interactions were showed between CPD1 and amino acid residues ALA41, ARG48, ASN84, LEU142, PHE45, TRP85, TYR49, TYR143 (Fig. 4A and 4B). 5-FU participated in hydrogen bonds within the binding

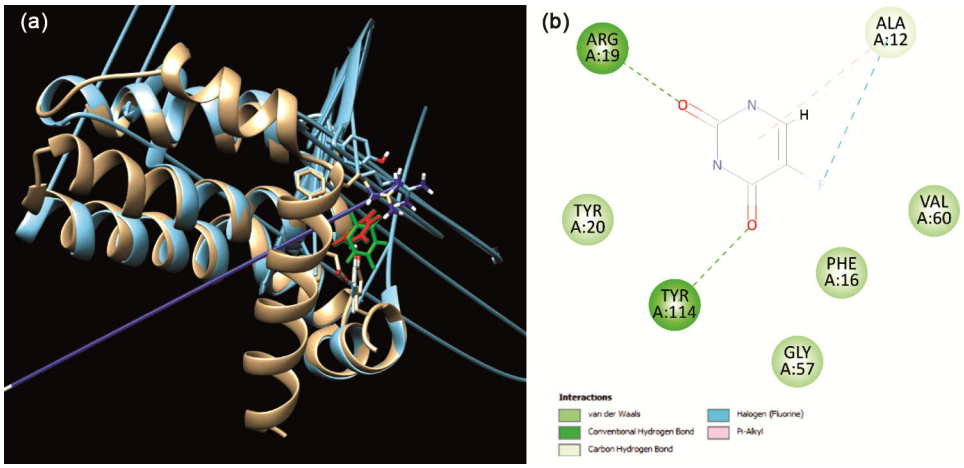

Fig. 5 — (A) Structural superposition of 5-FU-6GL8 docked complex before molecular dynamic (0 ps, green) and after molecular dynamic (10000 ps, red). (B) Interactions schematic after 10000 ps molecular dynamic simulation.

site of 6GL8 with amino acid residues ALA12, ARG19 and TYR144. It also engaged in a halogen bond and alkyl-π interaction with amino acid residue ALA12. The ligand was surrounded by van der Waals interactions with amino acid residues GLY57, PHE16, TYR20, and VAL60 (Fig. 5A and 5B).

Based on the evidence above, it could be concluded that the molecular dynamics simulation results reveal a persistent inhibition mode and consistent binding interactions in all simulations. These findings indicated that the binding of CPD1 to the 6GL8 receptor was stable throughout the simulation. These results support the reliability and credibility of this study's molecular dynamics simulation approach. CPD1 could be a good candidate for new inhibitors of anti-apoptotic BCL-2 proteins in colorectal cancer.

References

1 Brown J S, Amend S R, Austin R H, Gatenby R A, Hammarlund E U & Pienta K J, *Mol Cancer Res*, 21 (2023) 1142.
2 Barry M A, Behnke C A & Eastman A, *Biochem Pharmacol*, 40 (1990) 2353.
3 Elmore S, *Toxicol Pathol*, 35 (2007) 495.
4 Czabotar P E, Lessene G, Strasser A & Adams J M, *Nat Rev Mol Cell Biol*, 15 (2014) 49.
5 Qian S, Wei Z, Yang W, Huang J, Yang Y & Wang J, *Front Oncol* 12 (2022) 985363.
6 Rezgui A, Mitaine-Offer A C, Miyamoto T, Tanaka C, Delemasure S, Dutartre P & Lacaille-Dubois M A, *Phytochemistry*, 123 (2016) 40.
7 Nguyen D H, Mitaine-Offer A C, Miyamoto T, Tanaka C, Bellaye P S, Collin B, Chambin O & Lacaille-Dubois M A, *Phytochem Lett*, 37 (2020) 85.
8 Nguyen D H, Mitaine-Offer A C, Maroso S, Papini A M, Paululat T, Bellaye P S, Collin B, Chambin O & Lacaille-Dubois M A, *Fitoterapia*, 137 (2019) 104242.
9 Won Y M, Seong Z K, Kim J L, Kim H S, Song H H, Kim D Y, Kim J H, Oh S R, Cho H W, Cho J H & Lee H K, *Arch Pharm Res*, 38 (2015) 1541.
10 Podolak I, Grabowska K, Sobolewska D, Wróbel-Biedrawa D, Makowska-Was J & Galanty A, *Phytochem Rev,* 22 (2023) 113.
11 Elekofehinti O O, Iwaloye O, Olawale F & Ariyo E O, *Pathophysiology*, 28 (2021) 250.
12 Casara P, Davidson J, Claperon A, Toumelin-Braizat G L, Vogler M, Bruno A, Chanrion M, Lysiak-Auvity G, Diguarher T L, Starck J B, Chen I, Whitehead N, Graham C, Matassova N, Dokurno P, Pedder C, Wang Y, Qiu S, Girard A M, Schneider E, Gravé F, Studeny A, Guasconi G, Rocchetti F, Maïga S, Henlin J M, Colland F, Kraus-Berthier L, Gouill S L, JS Dyer M, Hubbard R, Wood M, Amiot M, Cohen G M, Hickman J A, Morris E, Murray J & Geneste O, *Oncotarget*, 9 (2018) 20075.
13 Van Der Spoel D, Lindahl E, Hess B, Groenhof G, Mark A E & Berendsen H J, *J Comput Chem,* 26 (2005) 1701.
14 Guex N & Peitsch M C, *Electrophoresis*, 18 (1997) 2714.
15 Zoete V, Cuendet M A, Grosdidier A & Michielin O, *J Comput Chem,* 32 (2011) 2359.
16 Pettersen E F, Goddard T D, Huang C C, Couch G S, Greenblatt D M, Meng E C & Ferrin T E, *J Comput Chem*, 25 (2004) 1605.
17 Bitencourt-Ferreira G, Veit-Acosta M & De Azevedo W F, *Van der Waals Potential in Protein Complexes*, (Springer, New York) 2019, p. 79.
18 Righetti P G & Boschetti E, *Chapter 4 - Low-Abundance Protein Access by Combinatorial Peptide Libraries*, (Elsevier, Boston) 2013, p. 79.
19 Lippert T & Rarey M, *J Cheminform*, 1 (2009) 1.
20 Jeong E, Kim H, Lee S W & Han K, *Mol Cells*, 16 (2003) 161.
21 Rhys N H, Soper A K & Dougan L, *J Phys Chem B*, 116 (2012) 13308.
22 Terefe E M & Ghosh A, *Bioinform Biol Insights*, 16 (2022) 11779322221125605.
23 Vaghasiya M D, Mendapara J V, Vaghasiya S P, Rajani D P, Ahmad I, Patel H & Kumari P, *J Mol Struct*, 1294 (2023) 136308.